

This paper is published as part of a *Dalton Transactions* themed issue entitled:

New Talent: Americas

Guest Editors: John Arnold, Dan Mindiola, Theo Agapie,
Jennifer Love and Mircea Dincă

Published in issue 26, 2012 of *Dalton Transactions*

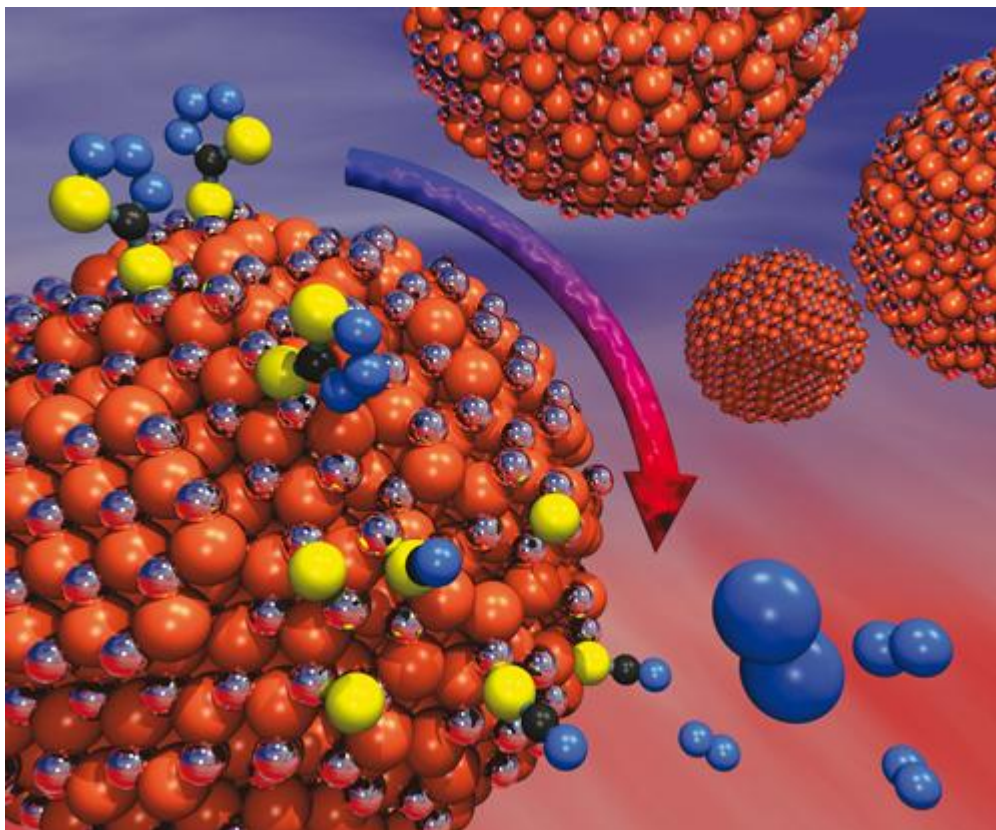


Image reproduced with permission of Richard L. Brutchey

Articles published in this issue include:

Synthesis and reactivity of 2-azametallacyclobutanes

Alexander Dauth and Jennifer A. Love

Dalton Trans., 2012, DOI: 10.1039/C2DT30639E

Perceiving molecular themes in the structures and bonding of intermetallic phases: the role of Hückel theory in an *ab initio* era

Timothy E. Stacey and Daniel C. Fredrickson

Dalton Trans., 2012, DOI: 10.1039/C2DT30298E

Cycloruthenated sensitizers: improving the dye-sensitized solar cell with classical inorganic chemistry principles

Kiyoshi C. D. Robson, Paolo G. Bomben and Curtis P. Berlinguette

Dalton Trans., 2012, DOI: 10.1039/C2DT30825H

Visit the *Dalton Transactions* website for more cutting-edge inorganic chemistry

www.rsc.org/dalton

Cite this: *Dalton Trans.*, 2012, **41**, 7920

www.rsc.org/dalton

PAPER

Cyclopentadienyl chromium diimine and pyridine-imine complexes:
ligand-based radicals and metal-based redox chemistry†Wen Zhou,^a Linus Chiang,^b Brian O. Patrick,^c Tim Storr^{*b} and Kevin M. Smith^{*a}

Received 20th January 2012, Accepted 16th April 2012

DOI: 10.1039/c2dt30160a

Paramagnetic CpCr(III) complexes with antiferromagnetically-coupled anionic radical diimine and pyridine-imine ligands were prepared and characterized. The diimine chloro CpCr[(ArNCR)₂]Cl complexes (**1**: Ar = 2,6-iPr₂C₆H₃ (Dpp), R = H; **2**: Ar = 2,6-Me₂C₆H₃ (Xyl), R = Me; **3**: Ar = 2,4,6-Me₃C₆H₂ (Mes), R = Me) were synthesized by treatment of previously reported Cr(diimine)(THF)₂Cl₂ precursors with NaCp. Reduction of **1** with Zn gives CpCr[(DppNCH)₂], **4**, resulting from reduction of Cr(III) to Cr(II) with retention of the ligand-based radical. Alkoxide complexes CpCr[(DppNCH)₂](OCR₂R') (**5**: R = Me, R' = Ph; **6**: R = iPr, R' = H) were synthesized by protonolysis of Cp₂Cr with HOOCR₂R' in the presence of the neutral diimine and catalytic base. The corresponding radical pyridine-imine complexes CpCr(PyCHNMe)Cl (**9**), CpCr(PyCHNMe) (**8**), and CpCr(PyCHNMe)(OCMe₂Ph) (**11**), were prepared by analogous routes. Oxidation of **8** with iodine gives CpCr(PyCHNMe)I (**10**) where oxidation of Cr(II) to Cr(III) again occurs with retention of the anionic pyridine-imine radical ligand. The molecular structures of complexes **1**, **2**, **4–8**, **10** and **11** were determined by single-crystal X-ray diffraction. Unusual low energy bands were observed in the UV-vis spectra of the reported complexes, with particularly strong transitions observed for the Cr(II) complexes **4** and **8**. The electronic structure of pyridine-imine complexes **8** and **10** were investigated by theoretical calculations.

Introduction

The tendency of certain classes of ligands to accept varying numbers of electrons from metals has long been recognized.¹ This “redox noninnocent behaviour” is particularly marked for first-row transition metals due to the energetic proximity of ligand and metal frontier electronic levels.² The development of highly active C–C bond forming catalysts for polymerization³ and organic synthesis⁴ using α -diimine, pyridine-imine, and 2,6-diiminepyridine ancillary ligands has naturally led to a resurgence of interest in these complexes.⁵

As our understanding of the connection between the electronic structure of such complexes and their reactivity has improved,⁶ different strategies have been developed for harnessing imines as ancillary ligands. Redox noninnocence has been employed to discourage radical reactivity in first row transition metal complexes in favour of more familiar two-electron reactivity modes.⁷

Alternatively, these ligands have been used to impart redox activity *via* ligand-based electron transfer, while the coordinated metal center maintains a constant oxidation state.⁸

Inert octahedral Cr(III) complexes display effective antiferromagnetic coupling between the unpaired d-electrons and ligand based radicals, such as semiquinonates.² Over 30 years ago, Tom Dieck prepared a neutral chromium bis(α -diimine) complex as a pre-catalyst for isoprene dimerization by reaction of Cr(acac)₃ with 2 equiv of the neutral diimine and 3 equiv of sodium metal.⁹ Most of the recent syntheses of chromium α -diimine complexes follow this route, reacting the neutral α -diimine with a reducing metal and a suitable chromium precursor, typically CrCl₂, CrCl₃, or CrCl₃(THF)₃.¹⁰ An interesting alternative synthetic strategy employed by Theopold and co-workers uses Cr(II) as the reducing agent by reacting the neutral α -diimine with CrCl₂ in THF.¹¹ The resulting Cr(α -diimine)(THF)₂Cl₂ complexes have a reduced radical anionic diimine ligand antiferromagnetically coupled to the Cr(III) center, and bear a striking structural resemblance to octahedral Cr(LX)(THF)₂Cl₂ Cr(III) complexes, where LX is a β -diketiminate or related non-radical bidentate monoanionic ligand,^{12,13} following Green's nomenclature for neutral (L) and anionic (X) donor atoms.¹⁴

Well-defined CpCr(LX) complexes with β -diketiminate ligands can be used to control the reactivity of carbon-based radicals *via* reversible Cr(III)–alkyl bond formation and homolysis.¹⁵ We were interested in using ligand-based radicals for this single electron chemistry, in order to facilitate metal-mediated radical reactivity rather than prevent it. Despite their superficial

^aDepartment of Chemistry, University of British Columbia Okanagan, 3333 University Way, Kelowna, BC, Canada V1V 1V7. E-mail: kevin.m.smith@ubc.ca

^bDepartment of Chemistry, Simon Fraser University, Burnaby, BC, Canada V5A 1S6. E-mail: tim_storr@sfu.ca

^cDepartment of Chemistry, University of British Columbia, Vancouver, BC, Canada V6T 1Z1

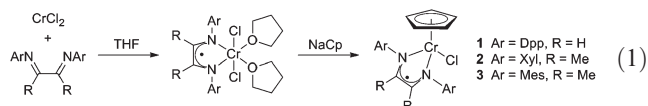
† Electronic supplementary information (ESI) available: Complete computational data, UV-vis spectra of complexes **1–11** and crystallographic data for complexes **1**, **2**, **4–8**, **10**, **11**. CCDC 864739–864747. For ESI and crystallographic data in CIF or other electronic format see DOI: 10.1039/c2dt30160a

structural similarities to β -diketiminate ligands, it was unclear if chromium-bound diimine ligand radicals would support the previously observed Cr(II)/Cr(III) chemistry, or if ligand-based electron transfer would occur instead. If the desired metal-based redox process was retained, α -diimine and pyridine-imine radical anionic ligands could provide access to CpCr(LX) complexes with enhanced reactivity. The direct reaction of Cr(II) precursors with neutral α -diimine ligands provided a potentially general and direct synthetic route to mixed-ligand Cr(III) complexes bearing anionic radical ligands.

Results and discussion

Synthesis of CpCr(α -diimine)Cl complexes

The new CpCr(α -diimine)Cl complexes were prepared by the two step synthetic route illustrated in eqn (1). Octahedral Cr(III) intermediates bearing ligand centered radicals were generated as previously reported by Theopold and co-workers,¹¹ by adding a neutral diimine ligand to a suspension of CrCl₂ in THF. Treatment of the brown dichloro intermediates with NaCp followed by recrystallization from hexanes gave the CpCr[(ArNCR)₂]Cl complexes (**1**: Ar = 2,6-iPr₂C₆H₃ (Dpp), R = H; **2**: Ar = 2,6-Me₂C₆H₃ (Xyl), R = Me; **3**: Ar = 2,4,6-Me₃C₆H₂ (Mes), R = Me) in moderate yields (eqn (1)).



The UV-vis spectra of complexes **1–3** were similar to the corresponding Cr(III) chloro complexes with β -diketiminate ligands, CpCr[(ArNCMe)₂CH]Cl with Ar = Dpp,¹⁶ Xyl,¹⁷ or Mes,¹⁸ consisting of a high intensity peak between 430 nm and 410 nm, and a lower intensity peak at \sim 575 nm. However, complexes **2** and **3** also exhibit an additional low intensity peak at \sim 650 nm not observed in the β -diketiminate complexes.

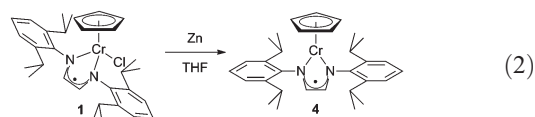
The three CpCr(α -diimine)Cl complexes have magnetic moments between 2.72 and 2.95 μ_B (Evans), corresponding to a $S = 1$ spin state. This is consistent with a paramagnetic low spin Cr(II) d^4 center with two unpaired electrons, although Wieghardt and co-workers have recently suggested that low-spin Cr(II) compounds may be much rarer than had previously been thought.¹⁹

The alternative electronic structure consistent with the experimental magnetic moments is Cr(III) (d^3 , $S = 3/2$) with strong antiferromagnetic coupling to an anionic ligand-based radical.^{11,19}

The molecular structures of **1** and **2** were determined by single crystal X-ray diffraction, and are shown in Fig. 1. The X-ray structures display bond lengths for the diimine ligands and structural parameters at the Cr centers consistent with radical anionic ligands bound to Cr(III). Since CpCr(acac)Br was synthesized over half a century ago,²⁰ related Cr(III) mono-halide complexes bearing both cyclopentadienyl and bidentate monoanionic ligands have been synthesized,^{16–18,21} including recently reported examples as olefin polymerization catalyst precursors.²² The structures of **1** and **2** are analogous to the related Cr(III) β -diketiminate species,^{16–18} although the decreased bite angles in **1** and **2** and the absence of backbone methyl groups in **1** both lead to reduced steric conflict between the bulky *N*-aryl substituents and the chloro ligand. The degree of steric repulsion in CpCr(III) β -diketiminate halide complexes has an apparent inverse relationship with the rates of oxidative addition of alkyl halides of the corresponding Cr(II) precursors.²³ Significantly, the α -diimine C–C bond lengths (1.387 Å for **1** and 1.397 Å for **2**) and C–N bond lengths (between 1.339 Å and 1.349 Å for both complexes) are all in the narrow ranges reported by Theopold and co-workers for anionic radical diimine ligands bound to Cr(II) and Cr(III).¹¹

Reduction of CpCr(DppNCH)₂Cl

Chemical reduction of **1** could potentially reduce either the metal center from Cr(III) to Cr(II), the radical anionic ligand to the spin-paired dianionic enediamide, or both. As shown in eqn (2), reaction of CpCr[(DppNCH)₂]Cl with Zn in THF followed by recrystallization from hexanes gives CpCr[(DppNCH)₂], (**4**), which has a magnetic moment of 3.78 μ_B (Evans).



The X-ray crystal structure of **4** (Fig. 2) is quite similar to the known CpCr(II) β -diketiminate complex CpCr[(DppNCH)₂CH].¹⁶

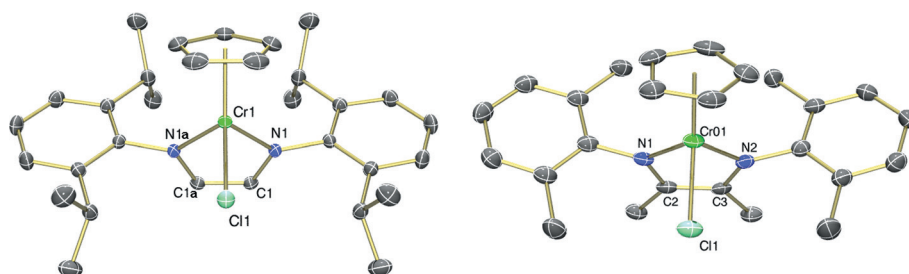


Fig. 1 Thermal ellipsoid diagrams (50%) of **1** (left) and **2** (right). For **1**, the atoms designated with an additional “a” in the atom labels are at equivalent position ($x, y, 1/2 - z$). Selected bond lengths (Å) and angles (°) for **1**: Cr(1)–N(1) = 1.966(1); N(1)–C(1) = 1.339(2); C(1)–C(1a) = 1.387(3); Cr(1)–Cl(1) = 2.277(6); N(1)–Cr(1)–Cl(1) = 93.73(4); N(1)–Cr(1)–N(1a) = 81.55(7). Selected bond lengths (Å) and angles (°) for **2**: Cr(01)–N(1) = 1.962(3); Cr(01)–N(2) = 1.962(3); N(1)–C(2) = 1.346(5); N(2)–C(3) = 1.348(5); C(2)–C(3) = 1.396(5); Cr(01)–Cl(1) = 2.301(1); N(1)–Cr(01)–Cl(1) = 96.70(9); N(2)–Cr(01)–Cl(1) = 97.10(9); N(1)–Cr(01)–N(2) = 80.1(1).

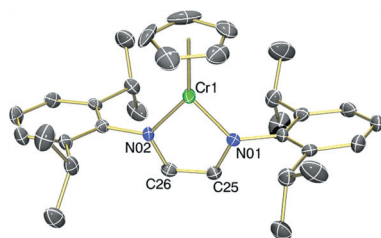


Fig. 2 Thermal ellipsoid diagram (50%) of **4**. Only one of the six independent molecules in the unit cell is shown. Selected bond lengths (Å) and angles (°): Cr(1)–N(01) = 1.933(3); Cr(1)–N(02) = 1.934(3); N(01)–C(25) = 1.362(4); N(02)–C(26) = 1.357(4); C(25)–C(26) = 1.356(4); N(01)–Cr(1)–N(02) = 81.3(1).

The six independent molecules of **4** in the unit cell have average C–C (1.358 Å) and C–N (1.361 Å) bond lengths that are again consistent with a radical diimine ligand.¹¹ The UV-vis spectrum of **4** displays a very strong absorbance at 670 nm that is not observed in related CpCr(II) β-diketiminato compounds. This prominent feature is convenient for spectroscopic monitoring of single-electron transfer reactions such as the chemical oxidation with PbCl₂ that cleanly converts **4** back to the Cr(III) chloride **1** (see ESI†). The conservation of the ligand-based diimine radical as the oxidation state of the chromium is altered has previously been noted,¹¹ and is in contrast to the reactivity observed for iron-bound pyridinediimine where redox processes can involve both the metal and the ligand.²⁴

Synthesis of CpCr[(DppNCH)₂](OR) by protonolysis of Cp₂Cr

Protonolysis reactions of Cp₂Cr are a useful route to new well-defined monomeric monocyclopentadienyl chromium derivatives.²⁵ Although chromocene reacts with *t*BuOH at elevated temperatures to give [CpCr(μ-OCMe₃)₂]₂,²⁶ the stable Cr₂(OR)₂ core remains intact even upon oxidation to Cr(III).²⁷ This renders [CpCr(μ-OCMe₃)₂]₂ unsuitable as a precursor to monomeric Cr–OR complexes. The synthesis of CpCr[(DppNCH)₂](OCR₂R') **5** (R = Me, R' = Ph) and **6** (R = *i*Pr, R' = H) as shown in eqn (3) was initially attempted to intercept a monomeric CpCr(OR) intermediate in the protonolysis of Cp₂Cr. The optimized protonolysis reaction to give **5** and **6** proceeds in good yields at room temperature, but the precise mechanism remains unclear. The accelerating effect observed upon addition of a catalytic amount of base, as seen in other protonolysis reactions,²⁸ suggests initial attack of an anionic ligand at Cp₂Cr to aid in cyclopentadienyl ligand displacement.²⁹ A similar effect may also be responsible for the halide-specific synthesis of CpM(L)X complexes by reaction of Cp₂M with substituted imidazolium halides (M = Ni, Cr),^{25,30–32} phosphonium chlorides (M = Ni),³¹ or DBU·HCl (M = Cr; DBU = 1,8-diazabicyclo[5.4.0]undec-7-ene).²⁵

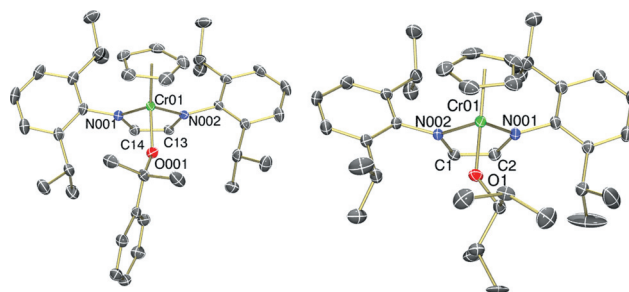
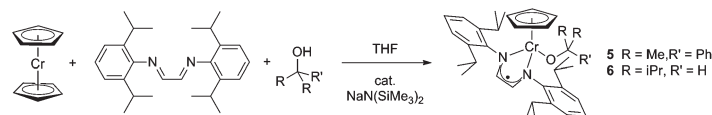
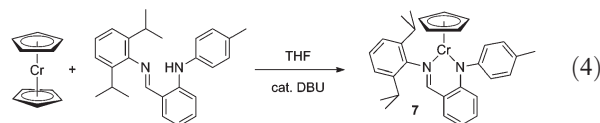


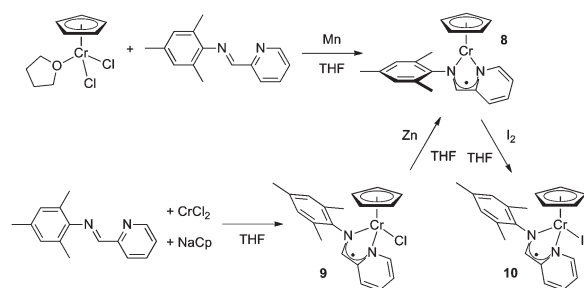
Fig. 3 Thermal ellipsoid diagrams (50%) of **5** (left) and **6** (right). Only one orientation of the disordered OCHiPr₂ ligand in **6** is shown. Selected bond lengths (Å) and angles (°) for **5**: Cr(01)–N(001) = 1.990(1); Cr(01)–N(002) = 1.994(1); N(001)–C(14) = 1.339(2); N(002)–C(13) = 1.341(2); C(13)–C(14) = 1.386(2); Cr(01)–O(001) = 1.886(1); N(001)–Cr(01)–O(001) = 96.04(5); N(001)–Cr(01)–N(002) = 80.88(5); N(002)–Cr(01)–O(001) = 93.61(4). Selected bond lengths (Å) and angles (°) for **6**: Cr(01)–N(001) = 1.978(1); Cr(01)–N(002) = 1.985(1); N(001)–C(2) = 1.344(2); N(002)–C(1) = 1.343(2); C(1)–C(2) = 1.386(2); Cr(01)–O(1) = 102.2(1); N(001)–Cr(01)–O(1) = 102.2(1); N(001)–Cr(01)–N(002) = 81.17(6); N(002)–Cr(01)–O(1) = 92.8(1).

The utility of catalytic base in the protonolysis of Cp₂Cr was also extended to anilido imine ligands.³³ The synthesis of CpCr[DppNCH(C₆H₄)NTol] (**7**) (Tol = 4-MeC₆H₄) was achieved by conducting the protonolysis at room temp with 22 mol% DBU as catalytic base (eqn (4)). The first Cr(III) anilido imine complexes were recently reported by Xu, Mu and co-workers.¹³ Single crystal X-ray diffraction of **7** showed a similar structure to analogous mixed aryl β-diketiminato CpCr(II) complexes, which were demonstrated to undergo faster single-electron oxidative addition reactions with MeI compared to the symmetric *ortho* disubstituted β-diketiminato derivatives.²³



The structures of the Cr(III) alkoxide complexes **5** and **6** were determined by X-ray diffraction and are shown in Fig. 3. As in Cr(III) chloride **1**, the average C–C (1.386 Å) and C–N (1.343 Å) bond lengths of the α-diimine groups are consistent with a radical anionic ligand.¹¹ Interestingly, Cr(II) complex **4** does not react with dicumyl peroxide at room temp to give **5**, presumably due to the steric bulk of the NDpp substituents hindering the inner sphere electron transfer process.

Reversible transfer of hydrogen from multidentate ancillary ligands to bound substrates has been recently recognized as a valuable ligand design feature.³⁴ A bound secondary alkoxide ligand, Cr–OCHR₂, could potentially transfer a hydrogen to one of the diimine carbon atoms in the ligand-based radical to

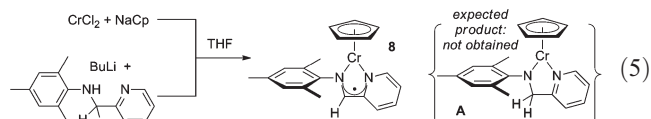


Scheme 1 Synthesis of pyridine-imine complexes.

generate a ketone and a non-radical amido imine ligand. Commercially available 2,4-dimethyl-3-pentanol is less sterically hindered than related alkoxide ligands recently employed in mid-valent chromium chemistry,³⁵ and the use of bulky and electron-donating $R = iPr$ substituents is expected to favour the H^\bullet transfer process both sterically and electronically. The $Cr-OCHiPr_2$ ligand in **6** was found to be disordered over two positions. In neither conformation was any interaction of the secondary alkoxide C–H bond with the ligand radical evident.

Attempted synthesis of $CpCr(PyCH_2NMe_3)$

To explore the potential for intramolecular H-atom transfer further, a route to an authentic $CpCr(II)$ complex with a redox innocent amido imine ligand was sought. Related pyridine amido ligands have been demonstrated to lead to highly selective Cr-based ethylene trimerization catalysts.³⁶ The attempted synthesis of $CpCr(PyCH_2NMe_3)$ (**A**) shown in eqn (5) followed the route previously used for $CpCr[(ArNCMe)_2CH]$ complexes, by treating $CrCl_2$ sequentially with first NaCp, and then the deprotonated ligand.¹⁸



The crystalline product isolated from this reaction unexpectedly displayed a very intense peak at 704 nm, similar to that observed for the $Cr(II)$ radical diimine complex **4**. A single crystal X-ray structure was obtained that confirmed the overall connectivity, although there was extensive disorder in the structure. Despite the disorder and poor data quality, the structure was more consistent with the radical complex resulting from loss of a ligand H atom, $CpCr(PyCHNMe_3)$, **8**, than the initial target pyridine amido complex **A**.

Synthesis of $CpCr(PyCHNMe_3)$ complexes

Radical pyridine-imine ligands have recently been investigated for first-row transition metals,³⁷ and for aluminum complexes.³⁸ An improved synthetic route to $CpCr(PyCHNMe_3)$, **8**, is shown in Scheme 1, consisting of Mn reduction of $CpCrCl_2(THF)$ in the presence of the neutral pyridine-imine ligand. The corresponding $Cr(III)$ Cl complex **9** is obtained by sequential treatment of $CrCl_2$ with $PyCHNMe_3$ and NaCp. Oxidation of **8** with

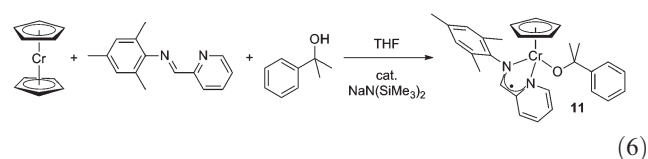
Table 1 Comparison of experimental and calculated^a bond lengths (in Å) for **8**

Method	Cr–N _{py}	Cr–N _{im}	Cr–Cp	C–C (ligand)	C–N (imine)
X-ray ^b	1.964	1.941	1.934	1.376	1.342
DFT (8 high spin $S = 5/2$)	2.073	2.065	2.007	1.412	1.345
DFT (8 $S = 3/2$)	2.021	1.989	1.979	1.399	1.355
DFT (A $S = 2$)	2.074	1.979	2.012	1.509	1.441

^a See Experimental section for details. ^b Average of two molecules in unit cell.

one-half equiv of I_2 gives the $Cr(III)$ iodide complex **10**, which was structurally characterized by X-ray diffraction, as shown in Fig. 4. Compared to the neutral pyridine-imine ligand, the relatively long imine C–N bond (1.344(2) Å) and short C–C bond (1.406(2) Å) in complex **10** are consistent with a singly reduced radical ligand.^{37,38} As was observed with the α -diimine complexes, single electron transfer reactions of these complexes lead to Cr-based redox chemistry while the radical ligand retains its unpaired electron, antiferromagnetically coupled to the paramagnetic metal center.

As shown in eqn (6), the $Cr(III)$ alkoxide complex $CpCr(PyCHNMe_3)(OCMe_2Ph)$, **11**, was prepared by protonolysis of chromocene, analogous to the synthesis of **5**. The X-ray crystal structure of **11** (Fig. 4) revealed a typical $Cr(III)$ half-sandwich $CpCr(LX)X$ geometry.^{16–18,20–22} The key imine C–N (1.339(2) Å) and C–C (1.404(2) Å) bond lengths are once again indicative of a radical anionic ligand.^{37,38}



Investigation of $CpCr(PyCHNMe_3)$ by theoretical calculations

In order to explore the electronic structure and UV-vis spectra of $CpCr(II)$ complexes bearing radical pyridine-imine ligands, density functional theory (DFT) calculations were employed. The geometry of $CpCr(PyCHNMe_3)$, **8**, was calculated in both the $S = 5/2$ and $S = 3/2$ spin states. For comparison, the geometry of the initial target pyridine amido complex $CpCr(PyCH_2NMe_3)$, **A**, was also optimized in the expected $S = 2$ spin state.

Although the coordination sphere metrical parameters for **A** are mostly within ± 0.1 Å of the experimental values, a significant difference ($+0.13$ Å) between the experimental and theoretical value for the pyridine-imine C–C bond is evident for **A**. These differences between calculated and observed bond lengths are reduced substantially for both the high spin ($S = 5/2$) and $S = 3/2$ solutions for **8** (Table 1). Overall, the $S = 3/2$ metrical parameters for **8** best fit the experimental data.

Using a hybrid functional the $S = 3/2$ solution for **8** is stabilized in comparison to the high spin ($S = 5/2$) state by *ca.* 8 kcal mol^{−1}, in agreement with the experimental magnetic data. The predicted $S = 3/2$ spin expectation value for **8** ($\langle S^2 \rangle = 4.47$)

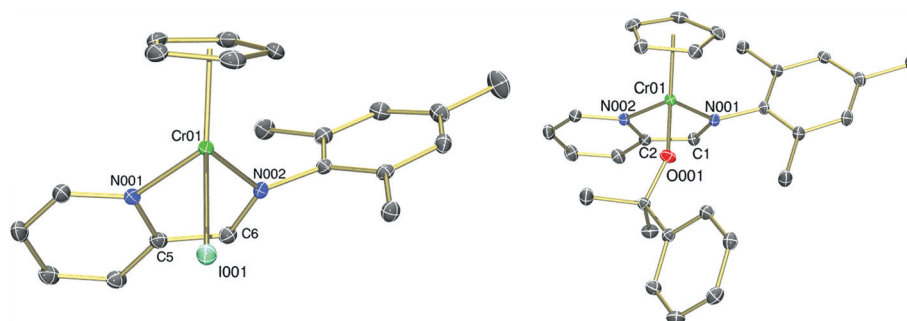


Fig. 4 Thermal ellipsoid diagram (50%) of **10** (left) and **11** (right). Selected bond lengths (Å) and angles (°) for **10**: Cr(01)–N(001) = 1.992(1); Cr(01)–N(002) = 1.968(1); N(001)–C(5) = 1.382(2); N(002)–C(6) = 1.344(2); C(5)–C(6) = 1.406(2); Cr(01)–I(001) = 2.6865(3); N(001)–Cr(01)–I(001) = 91.83(4); N(001)–Cr(01)–N(002) = 80.00(5); N(002)–Cr(01)–I(001) = 102.43(4). Selected bond lengths (Å) and angles (°) for **11**: Cr(01)–N(001) = 1.975(1); Cr(01)–N(002) = 1.988(1); N(001)–C(1) = 1.339(2); N(002)–C(2) = 1.388(2); C(1)–C(2) = 1.404(2); Cr(01)–O(001) = 1.880(1); N(001)–Cr(01)–O(001) = 103.35(5); N(001)–Cr(01)–N(002) = 79.54(5); N(002)–Cr(01)–O(001) = 100.75(4).

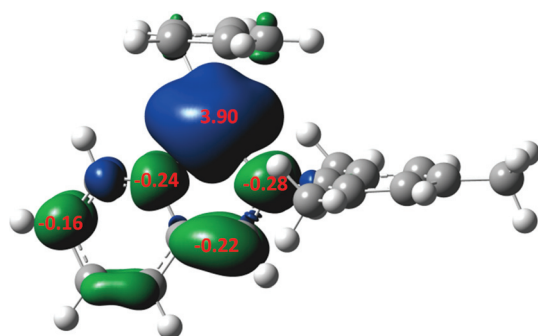


Fig. 5 Spin density plot for **8** showing the antiferromagnetic coupling between the Cr(II) ion and the imino-pyridine ligand radical. Mulliken spin densities shown in red.

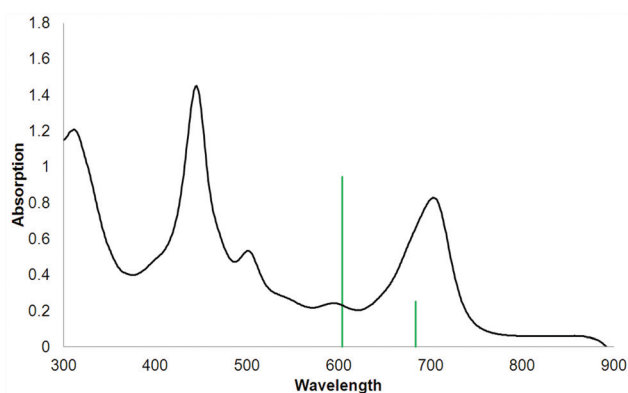


Fig. 6 UV-vis absorption spectra of **8** (black line), 1.32×10^{-4} M in hexanes. Calculated low energy transitions are shown in green for the $S = 3/2$ solution.

indicates *ca.* 15% spin contamination by the high spin state.³⁹ The computed spin expectation value demonstrates a considerable bonding interaction between the metal centre and the ligand radical, providing further evidence for antiferromagnetic coupling in the ground state.⁴⁰ A spin density plot for **8** is shown in Fig. 5 and displays the predicted antiferromagnetic coupling interaction between Cr(II) d^4 ion and the pyridine-imine ligand radical.

Table 2 TD-DFT^a predicted low energy bands for **8**

Transition (MO number)	Predicted transitions (nm)	Oscillator strength (<i>f</i>) (predicted)	Assignment ^b
α -HOMO \rightarrow α -LUMO	604	0.0947	MLCT
β -HOMO \rightarrow β -LUMO	684	0.0251	Intra-ligand

^a $S = 3/2$ solution, see text for details. ^b Assignment by AOMIX decomposition of relevant MOs into constituent components.^{43–45}

UV-vis spectroscopy of compound **8** in hexane displays a relatively intense transition at low energy (Fig. 6 and Table 2). We employed time-dependent DFT (TD-DFT)^{41,42} to better understand the nature of the low energy band, and in addition delineate between the possible structural and electronic forms of compound **8**, although it should be noted that TD-DFT computed intensities using a mixed spin state solution should be treated with caution. TD-DFT calculations on the high-spin ($S = 5/2$) electronic structure for **8** (as well as the target molecule **A**) do not predict any low energy transitions of appreciable intensity ($f > 0.02$) at wavelengths longer than 400 nm (see ESI†). The $S = 3/2$ solution predicts two bands at low energy as shown in Fig. 5. Even though the most intense band is blue-shifted in comparison to the experimental transition, this result provides further support for an antiferromagnetic ($S = 3/2$) ground state for **8**.

Analysis of the predicted bands in terms of the molecular orbitals involved, allows for the assignment of the most intense low energy band as a metal to ligand charge transfer (MLCT) band (Table 2). This is predominantly the α -HOMO \rightarrow α -LUMO transition (Fig. 7), in which the chromium metal character decreases substantially in the α -LUMO based on analysis of the compositions of the MOs.^{43–45} The α -HOMO \rightarrow α -LUMO transition is thus predicted to involve the transfer of electron density from Cr to the pyridine-imine ligand radical. The less intense β -HOMO \rightarrow β -LUMO transition is not as straightforward to assign and we have tentatively labeled as an intra-ligand transition of the pyridine-imine ligand radical based on orbital analysis, similar to related transitions observed by the groups of Wieghardt and Berben.^{37,38}

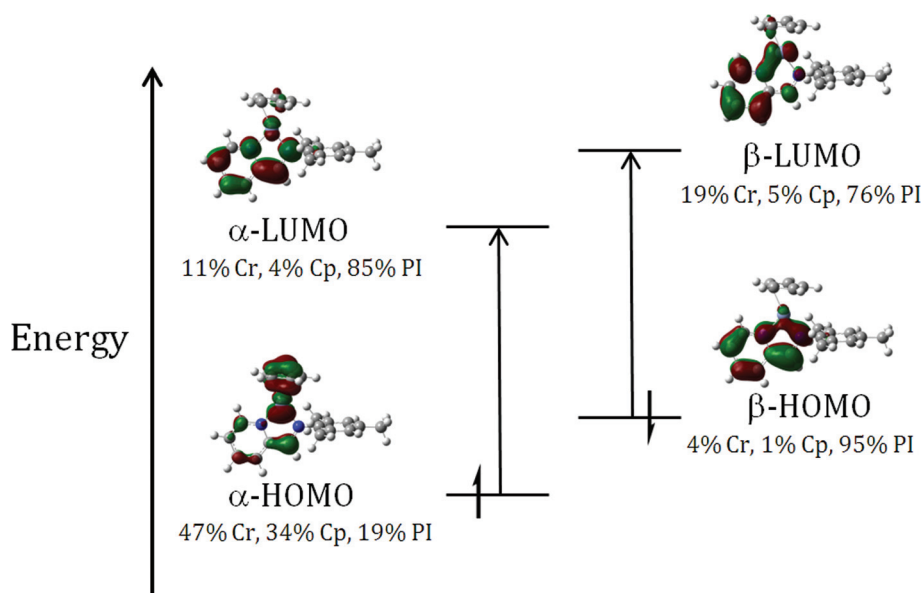


Fig. 7 Partial Kohn-Sham molecular orbital diagram for the $S = 3/2$ solution for **8** and TD-DFT assignment of the low energy transitions at 604 nm (α -HOMO \rightarrow α -LUMO) and 684 nm (β -HOMO \rightarrow β -LUMO). Molecular orbital compositions calculated using AOMIX.^{43–45} See Experimental section for details.

Table 3 Comparison of experimental and calculated^a bond lengths (in Å) for **10**

Method	Cr–N _{py}	Cr–N _{imine}	Cr–Cp	Cr–I	C–C (ligand)	C–N (imine)
X-ray	1.992	1.968	1.887	2.686	1.406	1.344
DFT (high spin $S = 2$)	2.048	2.057	1.938	2.722	1.406	1.351
DFT (broken symmetry $S = 1$)	2.017	1.999	1.931	2.736	1.406	1.346

^a See Experimental section for details.

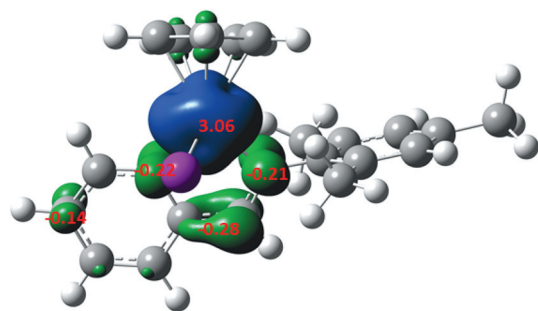


Fig. 8 Spin density plot for **10** showing the antiferromagnetic coupling between the Cr(III) ion and the pyridine-imine ligand radical. Mulliken spin densities shown in red.

Investigation of CpCr(PyCHNMe)sI by theoretical calculations

DFT calculations on **10** allowed for a comparison of the X-ray metrical parameters with the optimized geometries in both spin states (Table 3). The predicted coordination sphere metrical parameters for both the high spin ($S = 2$) and triplet ($S = 1$)

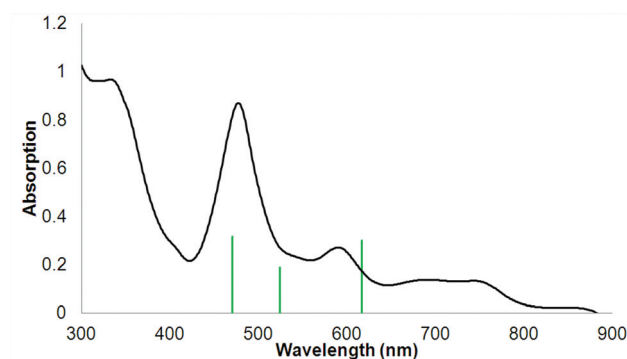


Fig. 9 UV-vis absorption spectra of **10** (black line), 1.24×10^{-4} M in hexanes. Calculated low energy transitions 470 nm, 524 nm, and 617 nm are shown in green for the $S = 1$ solution.

solutions are within ± 0.06 Å of the experimental values. Overall, the $S = 1$ metrical parameters for **10** are a slightly better fit with the experimental metrical data.

Using a hybrid functional the $S = 1$ solution for **10** is stabilized in comparison to the high spin ($S = 2$) state by *ca.* 5 kcal mol^{−1}, in agreement with experimental magnetic data. This energy difference is less than that predicted for compound **8**. The predicted $S = 1$ spin expectation value for **10** ($\langle S^2 \rangle = 2.78$) indicates *ca.* 20% spin contamination by the high spin state.³⁹ The computed spin expectation value demonstrates a considerable bonding interaction between the metal centre and the ligand radical, providing further evidence for antiferromagnetic coupling in the ground state.⁴⁰ A spin density plot for **10** is shown in Fig. 8 and displays the predicted antiferromagnetic coupling interaction between the Cr(III) d³ ion and the pyridine-imine ligand radical in the ground state.

UV-vis spectroscopy of compound **10** in hexane displays a series of weak transitions at low energy (Fig. 9 and Table 4), in contrast to the relatively intense band present at 700 nm for **8**.

TD-DFT analysis of the $S = 1$ solution for **10** predicts three transitions >400 nm of appreciable intensity at 470 nm, 524 nm, and 617 nm as detailed in Table 4. Analysis of the predicted bands in terms of the molecular orbitals involved allows for the assignment of the transitions at 524 nm and 617 nm as ligand to metal

Table 4 Comparison of the experimental and predicted TD-DFT^a low energy transitions for **10**

Transition (MO number)	Predicted transitions	Oscillator strength (<i>f</i>) (predicted)	Assignment ^b
α -HOMO \rightarrow α -LUMO	470	0.0316	LLCT
β -HOMO \rightarrow β -LUMO + 3	524	0.0188	LMCT
β -HOMO \rightarrow β -LUMO + 2	617	0.0299	LMCT

^a $S = 1$ solution, see text for details. ^b Assignment by AOMIX decomposition of relevant MOs into constituent components.^{43–45}

charge transfer (LMCT) bands. In both cases electron density is transferred from the pyridine-imine ligand radical to the Cr(III) ion (Fig. 10). The higher energy transition at 470 nm is predicted to be a LLCT band with the transfer of electron density from the Γ^- ligand to the pyridine-imine ligand radical. The higher charge of the Cr(III) ion in **10** eliminates the intense MLCT transition predicted for **8** (containing Cr(II)), matching the experimental UV-vis spectra for the two compounds.

Conclusions

The reaction of Cr(II) species with neutral α -diimine or pyridine-imine ligands is a useful synthetic route to mixed-ligand complexes bearing radical anionic ligands with antiferromagnetic coupling to the Cr(III) center. Chemical reduction and re-oxidation of CpCr(III) halide complexes results in metal-based redox while retaining an unpaired ligand-based electron. Structural characterization of the new complexes by single-crystal X-ray diffraction reveal half-sandwich chromium complexes that at least superficially resemble CpCr(LX) and CpCr(LX)X compounds with β -diketiminato ligands. The crystal structures also

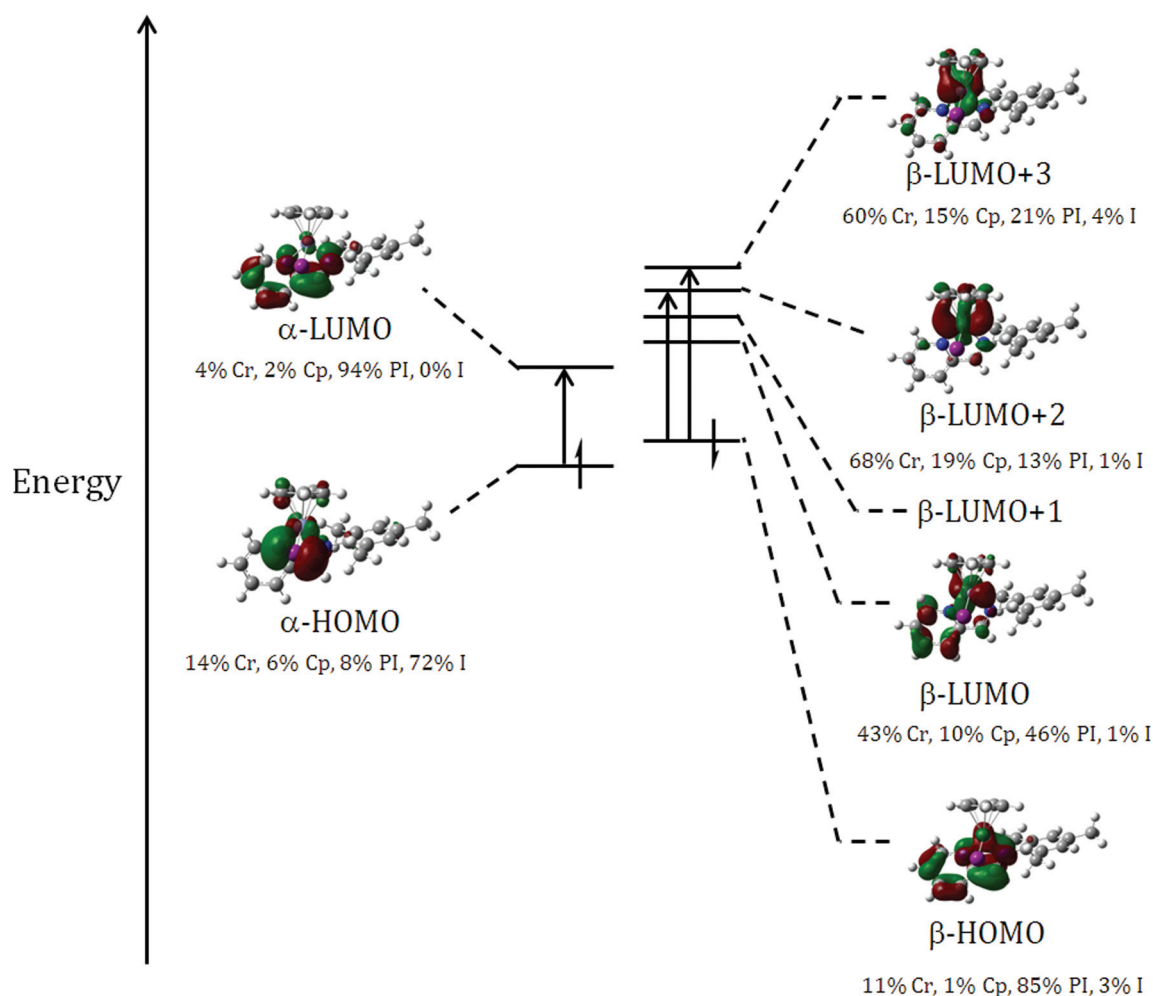


Fig. 10 Partial Kohn-Sham molecular orbital diagram for the $S = 1$ solution for **10** and TD-DFT assignment of the low energy transitions at 470 nm (α -HOMO \rightarrow α -LUMO), 524 nm (β -HOMO \rightarrow β -LUMO + 3), and 617 nm (β -HOMO \rightarrow β -LUMO + 2). Molecular orbital compositions calculated using AOMIX.^{43–45} See Experimental section for details.

show the shortened C–C bonds and elongated C–N bonds typical of α -diimine or pyridine-imine ligand radicals. The new complexes display distinctive bands at higher wavelengths in their UV-vis spectra than the corresponding compounds with non-radical β -diketiminato ligands. The low energy band is particularly intense for the CpCr(II) complexes with α -diimine or pyridine-imine ligand radicals, and provides a convenient peak for monitoring reactions by UV-vis spectroscopy. Density functional theory calculations support the proposed electronic structure of the Cr(II) and Cr(III) pyridine-imine complexes, and TD-DFT calculations demonstrate the involvement of the ligand-based radicals in the distinctive high intensity, lower energy bands in the UV-vis spectra.

The inadvertent conversion of protonated PyCH₂NHMe to a radical pyridine-imine complex may have implications for the nature of the catalytic species in the selective Cr-catalyzed trimerization of ethylene using related ligand precursors.³⁶ An isolated complex with a bulky Cr-bound secondary alkoxide appeared to be stable with respect to intramolecular H-atom transfer to the diimine radical ligand. However, preliminary attempts in this laboratory to use these complexes as synthetic precursors to Cr(III) alkyl complexes have been complicated by unwanted ligand alkylation reactions. These initial results support the recent observations of Theopold and co-workers that their propensity for alkylation may limit the efficacy of α -diimines as ancillary ligands in organochromium chemistry.⁴⁶

Experimental section

General considerations

All reactions were carried out under nitrogen using standard Schlenk and glove box techniques. Solvents were dried by using the method of Grubbs.⁴⁷ Celite (Aldrich) was dried overnight at 120 °C before being evacuated and then stored under nitrogen. Iodine was purified by sublimation, and 2,4-dimethyl-3-pentanol (99%, Aldrich) and DBU (1,8-diazabicyclo[5.4.0]undec-7-ene, 98%, Aldrich) were freeze-pump-thaw degassed before use. *p*-Toluenesulfonic acid monohydrate, 2-phenyl-2-propanol (97%), CrCl₂ (99% anhydrous), CrCl₃ (anhydrous), Zn (99% powder), Mn (99% powder), NaN(SiMe₃)₂, *n*-BuLi (1.6 M in hexanes), NaCp (2.0 M in THF), and 1,4-dioxane (anhydrous) were purchased from Aldrich and used as received. (ArNCR)₂,⁴⁸ PyCHNMe₅,⁴⁹ PyCH₂NHMe₅,⁵⁰ TolNHC₆H₄CHNDpp,³³ CpCr₂,⁵¹ and CpCr(THF)Cl₂⁵² were prepared according to the literature procedures.

UV-vis spectroscopic data were collected on a Varian Cary 100 Bio UV-visible or a Shimadzu UV 2550 UV-vis spectrophotometer in hexanes solution in a specially constructed cell for air-sensitive samples: a Kontes Hi-Vac Valve with PTFE plug was attached by a professional glassblower to a Hellma 10 mm path length quartz absorption cell with a quartz-to-glass graded seal. Elemental analyses were performed by Guelph Chemical Laboratories, Guelph, ON, Canada or by the UBC Department of Chemistry microanalytical services.

Computational details

Geometry optimizations were performed using the Gaussian 09 program (Revision A.02),⁵³ the B3LYP^{54,55} functional, and the

6-31G(d) basis set on all atoms except iodine which was modelled with the LanL2DZ^{56–58} basis set. Frequency calculations at the same level of theory confirmed that the optimized structures were located at a minimum on the potential energy surface. Single point calculations were performed using the B3LYP^{54,55} functional and the TZVP basis set of Ahlrichs^{59,60} on all atoms except iodine which was modeled with the LanL2DZ basis set. The intensities of the 30 lowest-energy electronic transitions were calculated by TD-DFT^{40,41} at the B3LYP/TZVP/LanL2DZ level with a polarized continuum model (PCM) for hexane.^{61–64} AOMIX^{43–45} was used for determining atomic orbital compositions employing Mulliken Population Analysis.

Synthesis of CpCr[(DppNCH)₂]Cl (1)

To a suspension of CrCl₂ (1.324 g, 10.76 mmol) in 30 mL THF, diimine (DppNCH)₂ (3.7949 g, 10.077 mmol) was added and stirred at room temperature for 20 h, during which time the colour changed from green to red. NaCp (5.5 mL, 2.0 M in THF, 11.0 mmol) was then added, causing the solution to become a dark green. After stirring for an additional 20 h, the solvent was removed *in vacuo*, the residue was extracted with 80 mL hexanes, and the dark green extracts were filtered through Celite, and cooled to –35 °C. Black crystals of **1** were isolated in two different fractions (2.322 g, 44%). (Evans, C₆D₆): 2.75 μ _B. Anal. Calcd for C₃₁H₄₁N₂CrCl: C, 70.37; H, 7.81; N, 5.29. Found: C, 70.84; H, 7.98; N, 5.24. UV/vis (hexanes; λ_{max} , nm (ϵ , M^{–1} cm^{–1})): 412 (8700), 567 (1300).

Synthesis of CpCr[(XylNCMe)₂]Cl (2)

To a suspension of CrCl₂ (171.0 mg, 1.390 mmol) in 20 mL THF, diimine (XylNCMe)₂ (405.7 mg, 1.387 mmol) was added and stirred at room temperature for 20 h, during which time the colour changed from green to red. NaCp (0.80 mL, 2.0 M in THF, 1.6 mmol) was then added, causing the solution to become a dark green. After stirring for an additional 20 h, the solvent was removed *in vacuo*, the residue was extracted with 9 mL hexanes, and then the dark green extracts were filtered through Celite and cooled to –35 °C. Black crystals of **2** were isolated in three different fractions (351.3 mg, 57%). (Evans, C₆D₆): 2.72 μ _B. Anal. Calcd for C₂₅H₂₉N₂CrCl: C, 67.48; H, 6.57; N, 6.29. Found: C, 68.06; H, 6.77; N, 6.13. UV/vis (hexanes; λ_{max} , nm (ϵ , M^{–1} cm^{–1})): 430 (6200), 580 (1000).

Synthesis of CpCr[(MesNCMe)₂]Cl (3)

To a suspension of CrCl₂ (151.2 mg, 1.229 mmol) in 20 mL THF, diimine (MesNCMe)₂ (403.8 mg, 1.260 mmol) was added and stirred at room temperature for 20 h, during which time the colour changed from green to red. NaCp (0.70 mL, 2.0 M in THF, 1.4 mmol) was then added, causing the solution to become a dark green. After stirring for an additional 20 h, the solvent was removed *in vacuo*, the residue was extracted with 7.5 mL hexanes, and then the dark green extracts were filtered through Celite and cooled to –35 °C. Black crystals of **3** were isolated in four different fractions (293.9 mg, 51%). (Evans, C₆D₆): 2.95 μ _B. Anal. Calcd for C₂₇H₃₃N₂CrCl: C, 68.56; H, 7.03; N,

5.92. Found: C, 69.18; H, 7.17; N, 6.00. UV/vis (hexanes; λ_{max} , nm (ϵ , $\text{M}^{-1} \text{cm}^{-1}$)): 420 (5500), 572 (900).

Synthesis of $\text{CpCr}[(\text{DppNCH})_2] \text{ (4)}$

To a solution of $\text{CpCr}[(\text{DppNCH})_2]\text{Cl}$ (101.6 mg, 0.206 mmol) in 15 mL THF, Zn (26.3 mg, 0.402 mmol) was added and stirred at room temperature for 20 h, during which the colour changed from green to blue. The solvent was removed *in vacuo*, the residue was extracted with 1 mL hexanes then filtered through Celite, and cooled to -35°C . Dark green crystals of **4** were isolated in one fraction (55.4 mg, 59%). (Evans, C_6D_6): 3.78 μB . Anal. Calcd for $\text{C}_{31}\text{H}_{34}\text{N}_2\text{Cr}$: C, 75.42; H, 8.37; N, 5.67. Found: C, 75.55; H, 8.43; N, 5.70. UV/vis (hexanes; λ_{max} , nm (ϵ , $\text{M}^{-1} \text{cm}^{-1}$)): 406 (5500), 532 (1700), 649 (4800).

Synthesis of $\text{CpCr}[(\text{DppNCH})_2]\text{OCMe}_2\text{Ph}$ (5)

To a solution of Cp_2Cr (50.5 mg, 0.277 mmol) in 5 mL THF, diimine $(\text{DppNCH})_2$ (116.2 mg, 0.308 mmol) was added. After stirring for 1 h, HOCMe_2Ph (44.3 mg, 0.325 mmol) and a catalytic amount of $\text{NaN}(\text{SiMe}_3)_2$ (<5 mg, <10 mol%) were dissolved in 3 mL THF and added to the Cp_2Cr solution. The resulting solution was stirred for 20 h, after which the solvent was removed from the dark green solution *in vacuo*. The residue was extracted with 3 mL of hexanes, filtered through Celite, and cooled to -35°C . Dark green crystals of **5** were isolated in three different fractions (113.8 mg, 65%). (Evans, C_6D_6): 2.65 μB . Anal. Calcd for $\text{C}_{40}\text{H}_{52}\text{N}_2\text{CrO}$: C, 76.40; H, 8.33; N, 4.45. Found: C, 76.14; H, 8.50; N, 4.44. UV/vis (hexanes; λ_{max} , nm (ϵ , $\text{M}^{-1} \text{cm}^{-1}$)): 437 (5700), 584 (800), 688 (600).

Synthesis of $\text{CpCr}[(\text{DppNCH})_2]\text{OCHiPr}_2$ (6)

To a solution of Cp_2Cr (48.2 mg, 0.265 mmol) in 7.5 mL THF, diimine $(\text{DppNCH})_2$ (116.5 mg, 0.309 mmol) was added. After stirring for 30 min, HOCHiPr_2 (45 μL , 0.321 mmol) and a catalytic amount of $\text{NaN}(\text{SiMe}_3)_2$ (<5 mg, <10 mol%) were dissolved in 3 mL of THF and added to the Cp_2Cr solution. The resulting solution was stirred for 20 h, after which the solvent was removed from the dark green solution *in vacuo*. The residue was extracted with 3 mL hexanes, filtered through Celite, and cooled to -35°C . Dark green crystals of **6** were isolated in three different fractions (82.8 mg, 51%). Anal. Calcd for $\text{C}_{38}\text{H}_{56}\text{N}_2\text{CrO}$: C, 74.96; H, 9.27; N, 4.60. Found: C, 75.23; H, 9.44; N, 4.73. UV/vis (hexane; λ_{max} , nm (ϵ , $\text{M}^{-1} \text{cm}^{-1}$)): 444 (5500), 568 (900), 702 (1000).

Synthesis of $\text{CpCr}(\text{ToINHC}_6\text{H}_4\text{CHNDpp})$ (7)

To a solution of Cp_2Cr (109.6 mg, 0.602 mmol) in 7.5 mL THF, the aniline imine $\text{ToINHC}_6\text{H}_4\text{CHNDpp}$ (251.42 mg, 0.680 mmol) and a catalytic amount of DBU (20 μL , 0.134 mmol) were added. The resulting dark red solution was stirred for 20 h, after which the solvent was removed *in vacuo*. The residue was extracted with 3 mL hexanes, filtered through Celite, and cooled to -35°C . Black crystals of **7** were isolated in two different fractions (131.0 mg, 45%). Anal. Calcd for

$\text{C}_{31}\text{H}_{34}\text{N}_2\text{Cr}$: C, 76.52; H, 7.04; N, 5.76. Found: C, 76.14; H, 7.34; N, 5.80. UV/vis (hexanes; λ_{max} , nm (ϵ , $\text{M}^{-1} \text{cm}^{-1}$)): 373 (6400), 493 (3600).

Synthesis of $\text{CpCr}(\text{PyCHNMe})$ (8)

To a solution of $\text{CpCr}(\text{THF})\text{Cl}_2$ (85.2 mg, 0.327 mmol) in 15 mL THF, a solution of the pyridine-imine PyCHNMe (90.6 mg, 0.404 mmol) in 3 mL of THF and Mn (430.1 mg, 7.828 mmol) were added. The suspension was stirred for 20 h, after which the solvent was removed *in vacuo*. The residue was extracted with 12 mL hexanes, filtered through Celite, and cooled to -35°C . Black crystals of **8** were isolated in two different fractions (51.2 mg, 56%). (Evans, C_6D_6): 3.63 μB . Anal. Calcd for $\text{C}_{20}\text{H}_{21}\text{N}_2\text{Cr}$: C, 70.37; H, 6.20; N, 8.20. Found: C, 70.56; H, 6.18; N, 8.15. UV/vis (hexanes; λ_{max} , nm (ϵ , $\text{M}^{-1} \text{cm}^{-1}$)): 445 (11 000), 502 (4100), 595 (1800), 704 (6300).

Synthesis of $\text{CpCr}(\text{PyCHNMe})\text{Cl}$ (9)

To a suspension of CrCl_2 (169.0 mg, 1.374 mmol) in 10 mL THF, the pyridine-imine PyCHNMe (300.5 mg, 1.340 mmol) was added and stirred at room temperature for 20 h. NaCp (0.70 mL, 2.0 M in THF, 1.4 mmol) was added, and the resulting black solution was stirred for 20 h. The solvent was then removed *in vacuo*, the residue was extracted with 15 mL hexanes, filtered through Celite, and cooled to -35°C . Black crystals of **9** were isolated in four different fractions (305 mg, 61%). (Evans, C_6D_6): 2.60 μB . Anal. Calcd for $\text{C}_{20}\text{H}_{21}\text{N}_2\text{CrCl}$: C, 63.74; H, 5.62; N, 7.43. Found: C, 63.70; H, 5.65; N, 7.24. UV/vis (THF; λ_{max} , nm (ϵ , $\text{M}^{-1} \text{cm}^{-1}$)): 471 (7000).

Synthesis of $\text{CpCr}(\text{PyCHNMe})\text{I}$ (10)

To a solution of $\text{CpCr}(\text{PyCHNMe})$ (45.8 mg, 0.134 mmol) in 7.5 mL Et_2O , was added I_2 (20.5 mg, 0.080 mmol) dissolved in 3 mL of Et_2O . After stirring for 20 h, the solvent was removed *in vacuo*, the residue was extracted with 3 mL Et_2O and 2 mL toluene filtered through Celite, and cooled to -35°C . Black crystals of **10** were isolated in two fractions (25.6 mg, 41%). Anal. Calcd for $\text{C}_{20}\text{H}_{21}\text{N}_2\text{CrI}$: C, 51.30; H, 4.52; N, 5.98. Found: C, 53.44; H, 5.36; N, 5.45. UV/vis (THF; λ_{max} , nm (ϵ , $\text{M}^{-1} \text{cm}^{-1}$)): 478 (7000), 591 (2100), 692 (1100), 743 (1100).

Synthesis of $\text{CpCr}(\text{PyCHNMe})\text{OCMe}_2\text{Ph}$ (11)

To a solution of Cp_2Cr (50.1 mg, 0.275 mmol) in 10 mL THF, the pyridine-imine PyCHNMe (68.3 mg, 0.304 mmol) was added. After stirring for 1 h, HOCMe_2Ph (43.2 mg, 0.317 mmol) and catalytic amount of $\text{NaN}(\text{SiMe}_3)_2$ (<5 mg, <10 mol%) dissolved of 3 mL THF were added. The solution was stirred for 20 h, after which the solvent was removed from the dark green solution *in vacuo*. The residue was extracted with 6 mL hexanes, filtered through Celite, and cooled to -35°C . Dark green crystals of **11** were isolated in one fraction (95.3 mg, 73%). (Evans, C_6D_6): 2.75 μB . Anal. Calcd for $\text{C}_{29}\text{H}_{32}\text{N}_2\text{CrO}$: C, 73.09; H, 6.77; N, 5.88. Found: C, 72.96; H, 7.00; N, 5.91.

UV/vis (hexanes; λ_{max} , nm (ϵ , $\text{M}^{-1} \text{cm}^{-1}$)): 413 (5500), 471 (6400), 612 (1800).

X-ray crystallography

Data collection. All crystals were mounted on a glass fiber and measurements were made on a Bruker X8 APEXII diffractometer with graphite-monochromated Mo $K\alpha$ radiation. The data were collected at a temperature of -100.0 ± 0.1 °C. Crystal data and refinement parameters are listed in the ESI.†

Data reduction. Data for all complexes were collected and integrated using the Bruker SAINT software package.⁶⁵ Data were corrected for absorption effects using the multiscan technique (SADABS)⁶⁶ unless otherwise mentioned below. The data were corrected for Lorentz and polarization effects.

Structure solution and refinement. The structures were solved by direct methods.⁶⁷ All non-hydrogen atoms were refined anisotropically (unless otherwise mentioned below). All hydrogen atoms were included in calculated positions but not refined (unless otherwise mentioned below). All refinements were performed using SHELXTL.⁶⁸ Compound **1** has a crystallographically-imposed mirror symmetry with the chromium, chlorine and C14 atoms on the mirror plane. The space group for compound **1**, *Pbnm*, is a non-standard setting of space group *Pnma*. For compound **2**, data were corrected for absorption effects using the multiscan technique (TWINABS).⁶⁹ The material crystallizes as a two-component split crystal with the two components related by 179.9° rotation about the (1 0 0) real axis. Data were integrated for both twin components. Subsequent refinements were carried out using an HKLF 4 format data set containing complete from component **1** and all overlapped reflections from component **2**. The batch scale refinement showed a roughly 54:46 ratio between the major and minor twin components. Compound **4** crystallizes with six independent molecules in the asymmetric unit, three of which contain a disordered Cp ligand that were subsequently modeled in two orientations. The one isopropyl substituent (C109, C110 and C111) in compound **4** was found to be disordered and was modeled in two orientations with 50% occupancy. All non-hydrogen atoms in compound **4** were refined anisotropically except for C1b, C2b, C3b, C4b, C7b, C8b, C9b, C10b, C11b, C12b, C13b, C14b, C15b, C17b and C18b. Compound **4** displays a Flack parameter of 0.49(1). A Flack parameter of approximately 0.5, in this case, is indicative of the pseudo- $P2_1/c$ symmetry of complex **4**. The alkoxide of compound **6** is disordered and was subsequently modeled in two orientations. All non-hydrogen atoms in compound **6** were refined anisotropically except for C33b. Compound **8** crystallizes with two independent molecules in the asymmetric unit, and displays a Flack parameter of 0.14(8). All non-hydrogen atoms in compound **8** were refined anisotropically except for C1, C2, C3, C4, C6, C8, C24, C27, C28, C29, C41 and N3.

Acknowledgements

We are grateful to the Natural Sciences and Engineering Research Council of Canada (NSERC), the Canadian Foundation for Innovation, and the University of British Columbia for

financial support. Compute Canada and Westgrid are thanked for access to computational resources.

References

- R. Eisenberg and H. B. Gray, *Inorg. Chem.*, 2011, **50**, 9741–9751; W. Kaim, *Inorg. Chem.*, 2011, **50**, 9752–9765.
- C. G. Pierpont, *Inorg. Chem.*, 2011, **50**, 9766–9772.
- F. Stoffelbach, R. Poli and P. Richard, *J. Organomet. Chem.*, 2002, **663**, 269–276; V. C. Gibson, R. K. O'Reilly, D. F. Wass, A. J. P. White and D. J. Williams, *Dalton Trans.*, 2003, 2824–2830; V. C. Gibson, C. Redshaw and G. A. Solan, *Chem. Rev.*, 2007, **107**, 1745–1776; T. Irrgang, S. Keller, H. Maisel, W. Kretschmer and R. Kempe, *Eur. J. Inorg. Chem.*, 2007, 4221–4228; H. Kaneko, H. Nagae, H. Tsurugi and K. Mashima, *J. Am. Chem. Soc.*, 2011, **133**, 19626–19629.
- K. T. Sylvester and P. J. Chirik, *J. Am. Chem. Soc.*, 2009, **131**, 8772–8774; S. K. Russell, J. M. Darmon, E. Lobkovsky and P. J. Chirik, *Inorg. Chem.*, 2010, **49**, 2782–2792; J. Y. Wu, B. N. Stanzl and T. Ritter, *J. Am. Chem. Soc.*, 2010, **132**, 13214–13216; A. M. Tondreau, C. C. H. Atienza, K. J. Weller, S. A. Nye, K. M. Lewis, J. G. P. Delis and P. J. Chirik, *Science*, 2012, **335**, 567–570.
- W. I. Dzik, J. I. van der Vlugt, J. N. H. Reek and B. de Bruin, *Angew. Chem., Int. Ed.*, 2011, **50**, 3356–3358.
- S. C. Bart, K. Chlopek, E. Bill, M. W. Bouwkamp, E. Lobkovsky, F. Neese, K. Wieghardt and P. J. Chirik, *J. Am. Chem. Soc.*, 2006, **128**, 13901–13912; Q. Knijnenburg, S. Gambarotta and P. H. M. Budzelaar, *Dalton Trans.*, 2006, 5442–5448; T. J. Dunn, C. F. Ramogida, C. Simmonds, A. Paterson, E. W. Y. Wong, L. Chiang, Y. Shimazaki and T. Storr, *Inorg. Chem.*, 2011, **50**, 6746–6755; C. C. Scarborough and K. Wieghardt, *Inorg. Chem.*, 2011, **50**, 9773–9793; D. Zhu, I. Thapa, I. Korobkov, S. Gambarotta and P. H. M. Budzelaar, *Inorg. Chem.*, 2011, **50**, 9879–9887; E. B. Hulley, P. T. Wolczanski and E. B. Lobkovsky, *J. Am. Chem. Soc.*, 2011, **133**, 18058–18061.
- P. J. Chirik and K. Wieghardt, *Science*, 2010, **327**, 794–795; A. L. Smith, K. I. Hardcastle and J. D. Soper, *J. Am. Chem. Soc.*, 2010, **132**, 14358–14360.
- N. A. Ketterer, H. Fan, K. J. Blackmore, X. Yang, J. W. Ziller, M.-H. Baik and A. F. Heyduk, *J. Am. Chem. Soc.*, 2008, **130**, 4364–4374; A. I. Nguyen, R. A. Zarkesh, D. C. Lacy, M. K. Thorson and A. F. Heyduk, *Chem. Sci.*, 2011, **2**, 166–169; A. F. Heyduk, R. A. Zarkesh and A. I. Nguyen, *Inorg. Chem.*, 2011, **50**, 9849–9863; R. A. Zarkesh and A. F. Heyduk, *Organometallics*, 2011, **30**, 4890–4898; H. Tsurugi, T. Saito, H. Tanahashi, J. Arnold and K. Mashima, *J. Am. Chem. Soc.*, 2011, **133**, 18673–18683.
- H. tom Dieck and A. Kinzel, *Angew. Chem., Int. Ed. Engl.*, 1979, **18**, 324–325.
- K. A. Kreisel, G. P. A. Yap, O. Dmitrenko, C. R. Landis and K. H. Theopold, *J. Am. Chem. Soc.*, 2007, **129**, 14162–14163; M. Ghosh, S. Sproules, T. Weyhermüller and K. Wieghardt, *Inorg. Chem.*, 2008, **47**, 5963–5970; I. L. Fedushkin, V. M. Makarov, V. G. Sokolov and G. K. Fukin, *Dalton Trans.*, 2009, 8047–8053; T. J. Knisley, M. J. Saly, M. J. Heeg, J. L. Roberts and C. H. Winter, *Organometallics*, 2011, **30**, 5010–5017; B. Gao, W. Gao, Q. Wu, X. Luo, J. Zhang, Q. Su and Y. Mu, *Organometallics*, 2011, **30**, 5480–5486; B. Gao, X. Luo, W. Gao, L. Huang, S. Gao, X. Liu, Q. Wu and Y. Mu, *Dalton Trans.*, 2012, **41**, 2755–2763.
- K. A. Kreisel, G. P. A. Yap and K. H. Theopold, *Inorg. Chem.*, 2008, **47**, 5293–5303.
- L. A. MacAdams, W.-K. Kim, L. M. Liable-Sands, I. A. Guzei, A. L. Rheingold and K. H. Theopold, *Organometallics*, 2002, **21**, 952–960; L. A. MacAdams, G. P. Buffone, C. D. Incarvito, A. L. Rheingold and K. H. Theopold, *J. Am. Chem. Soc.*, 2005, **127**, 1082–1083.
- T. Xu, H. An, W. Gao and Y. Mu, *Eur. J. Inorg. Chem.*, 2010, 3360–3364.
- M. L. H. Green, *J. Organomet. Chem.*, 1995, **500**, 127–148.
- K. C. MacLeod, J. L. Conway, B. O. Patrick and K. M. Smith, *J. Am. Chem. Soc.*, 2010, **132**, 17325–17334; K. C. MacLeod, B. O. Patrick and K. M. Smith, *Organometallics*, 2010, **29**, 6639–6641.
- J. C. Doherty, K. H. D. Ballem, B. O. Patrick and K. M. Smith, *Organometallics*, 2004, **23**, 1487–1489.
- Y. Champouret, K. C. MacLeod, U. Baisch, B. O. Patrick, K. M. Smith and R. Poli, *Organometallics*, 2010, **29**, 167–176.
- K. C. MacLeod, J. L. Conway, L. Tang, J. J. Smith, L. D. Corcoran, K. H. D. Ballem, B. O. Patrick and K. M. Smith, *Organometallics*, 2009, **28**, 6798–6806.

- 19 C. C. Scarborough, S. Sproules, T. Weyhermüller, S. DeBeer and K. Wieghardt, *Inorg. Chem.*, 2011, **50**, 12446–12462.
- 20 J. C. Thomas, *Chem. Ind.*, 1956, 1388.
- 21 L. E. Manzer, *Inorg. Chem.*, 1978, **17**, 1552–1558; D. S. Richeson, J. F. Mitchell and K. H. Theopold, *J. Am. Chem. Soc.*, 1987, **109**, 5868–5870; D. S. Richeson, J. F. Mitchell and K. H. Theopold, *Organometallics*, 1989, **8**, 2570–2577; O. Heinemann, P. W. Jolly, C. Krüger and G. P. J. Verhovnik, *J. Organomet. Chem.*, 1998, **553**, 477–479; S. L. Kuan, W. K. Leong, R. D. Webster and L. Y. Goh, *Organometallics*, 2012, **31**, 273–281.
- 22 T. Xu, Y. Mu, W. Gao, J. Ni, L. Ye and Y. Tao, *J. Am. Chem. Soc.*, 2007, **129**, 2236–2237; Y.-B. Huang and G.-X. Jin, *Dalton Trans.*, 2009, 767–769; Y.-B. Huang, W.-B. Yu and G.-X. Jin, *Organometallics*, 2009, **28**, 4170–4174.
- 23 W. Zhou, L. Tang, B. O. Patrick and K. M. Smith, *Organometallics*, 2011, **30**, 603–610.
- 24 A. M. Tondreau, C. Milsman, E. Lobkovsky and P. J. Chirik, *Inorg. Chem.*, 2011, **50**, 9888–9895.
- 25 W. Zhou, J. A. Therrien, D. L. K. Wence, E. N. Yallits, J. L. Conway, B. O. Patrick and K. M. Smith, *Dalton Trans.*, 2011, **40**, 337–339.
- 26 M. H. Chisholm, F. A. Cotton, M. W. Extine and D. C. Rideout, *Inorg. Chem.*, 1979, **18**, 120–125.
- 27 S. E. Nefedov, A. A. Pasynskii, I. L. Eremenko, B. Orasakhatov, O. G. Ellert, V. M. Novotortsev, S. B. Katsner, A. S. Antsyshkina and M. A. Porai-Koshits, *J. Organomet. Chem.*, 1988, **345**, 97–104.
- 28 A. Shafir and J. Arnold, *Inorg. Chim. Acta*, 2003, **345**, 216–220.
- 29 K. Jonas, *Angew. Chem., Int. Ed. Engl.*, 1985, **24**, 295–311; R. M. Buck, N. Vinayavekhin and R. F. Jordan, *J. Am. Chem. Soc.*, 2007, **129**, 3468–3469.
- 30 M. H. Voges, C. Romming and M. Tilset, *Organometallics*, 1999, **18**, 529–533.
- 31 R. A. Kelly III, N. M. Scott, S. Diez-Gonzalez, E. D. Stevens and S. P. Nolan, *Organometallics*, 2005, **24**, 3442–3447.
- 32 V. Ritleng, C. Barth, E. Brenner, S. Milosevic and M. J. Chetcuti, *Organometallics*, 2008, **27**, 4223–4228.
- 33 P. G. Hayes, G. C. Welch, D. J. H. Emslie, C. L. Noack, W. E. Piers and M. Parvez, *Organometallics*, 2003, **22**, 1577–1579; X. Liu, W. Gao, Y. Mu, G. Li, L. Ye, H. Xia, Y. Ren and S. Feng, *Organometallics*, 2005, **24**, 1614–1619.
- 34 K. Gunanathan and D. Milstein, *Acc. Chem. Res.*, 2011, **44**, 588–602; J. I. van der Vlugt, *Eur. J. Inorg. Chem.*, 2012, 363–375.
- 35 L. E. Manzer, *J. Am. Chem. Soc.*, 1978, **100**, 8068–8073; A. Kayal and S. C. Lee, *Inorg. Chem.*, 2002, **41**, 321–330; O. L. Sydora, P. T. Wolczanski, E. B. Lobkovsky, C. Buda and T. R. Cundari, *Inorg. Chem.*, 2005, **44**, 2606–2618; O. L. Sydora, D. S. Kuiper, P. T. Wolczanski, E. B. Lobkovsky, A. Dinescu and T. R. Cundari, *Inorg. Chem.*, 2006, **45**, 2008–2021; S. Groysman, D. Villagran and D. G. Nocera, *Inorg. Chem.*, 2010, **49**, 10759–10761; M. Sun, Y. Mu, Y. Liu, Q. Wu and L. Ye, *Organometallics*, 2011, **30**, 669–675; P. Qiu, R. Cheng, B. Liu, B. Tumanskii, R. J. Batrice, M. Botoshansky and M. S. Eisen, *Organometallics*, 2011, **30**, 2144–2148.
- 36 D. S. McGuinness, *Chem. Rev.*, 2011, **111**, 2321–2341.
- 37 C. C. Lu, E. Bill, T. Weyhermüller, E. Bothe and K. Wieghardt, *J. Am. Chem. Soc.*, 2008, **130**, 3181–3197; C. C. Lu, S. DeBeer George, T. Weyhermüller, E. Bill, E. Bothe and K. Wieghardt, *Angew. Chem., Int. Ed.*, 2008, **47**, 6384–6387.
- 38 T. W. Myers, N. Kazem, S. Stoll, R. D. Britt, M. Shanmugam and L. A. Berben, *J. Am. Chem. Soc.*, 2011, **133**, 8662–8672; T. W. Myers and L. A. Berben, *J. Am. Chem. Soc.*, 2011, **133**, 11865–11867; T. W. Myers and L. A. Berben, *Inorg. Chem.*, 2012, **51**, 1480–1488.
- 39 L. Noodleman, *J. Chem. Phys.*, 1981, **74**, 5737–5743; J. E. McGrady, R. Stranger and T. Lovell, *J. Phys. Chem. A*, 1997, **101**, 6265–6272.
- 40 A. B. P. Lever, *Coord. Chem. Rev.*, 2010, **254**, 1397–1405; S. D. J. McKinnon, B. O. Patrick, A. B. P. Lever and R. G. Hicks, *J. Am. Chem. Soc.*, 2011, **133**, 13587–13603.
- 41 M. E. Casida, *Recent Advances in Density Functional Methods*, ed. D. P. Chong, World Scientific, Singapore, 1995, p. 155.
- 42 R. E. Stratmann, G. E. Scuseria and M. J. Frisch, *J. Chem. Phys.*, 1998, **109**, 8218–8224.
- 43 S. I. Gorelsky, *AOMix: Program for Molecular Orbital Analysis*, <http://www.sg-chem.net/>, University of Ottawa, Canada, 2007.
- 44 S. I. Gorelsky and A. B. P. Lever, *J. Organomet. Chem.*, 2001, **635**, 187–196.
- 45 S. I. Gorelsky and E. I. Solomon, *Theor. Chem. Acc.*, 2008, **119**, 5–67.
- 46 K. A. Kreisel, G. P. A. Yap and K. H. Theopold, *Eur. J. Inorg. Chem.*, 2012, 520–529.
- 47 A. B. Pangborn, M. A. Giardello, R. G. Grubbs, R. K. Rosen and F. J. Timmers, *Organometallics*, 1996, **15**, 1518–1520.
- 48 M. B. Abrams, B. L. Scott and R. T. Baker, *Organometallics*, 2000, **19**, 4944–4956.
- 49 C. Burstein, C. W. Lehmann and F. Glorius, *Tetrahedron*, 2005, **61**, 6207–6217.
- 50 Z. Huang, K. Song, F. Liu, J. Long, H. Hu, H. Gao and Q. Wu, *J. Polym. Sci., Part A: Polym. Chem.*, 2008, **46**, 1618–1628.
- 51 R. B. King, *Organometallic Syntheses*, Academic Press, New York, NY, 1965, vol. 1, pp. 66–67.
- 52 A. Fürstner and N. Shi, *J. Am. Chem. Soc.*, 1996, **118**, 12349–12357.
- 53 M. J. Frisch, G. W. Trucks, H. B. Schlegel, G. E. Scuseria, M. A. Robb, J. R. Cheeseman, G. Scalmani, V. Barone, B. Mennucci, G. A. Petersson, H. Nakatsuji, M. Caricato, X. Li, H. P. Hratchian, A. F. Izmaylov, J. Bloino, G. Zheng, J. L. Sonnenberg, M. Hada, M. Ehara, K. Toyota, R. Fukuda, J. Hasegawa, M. Ishida, T. Nakajima, Y. Honda, O. Kitao, H. Nakai, T. Vreven, J. A. Montgomery Jr., J. E. Peralta, F. Ogliaro, M. Bearpark, J. J. Heyd, E. Brothers, K. N. Kudin, V. N. Staroverov, R. Kobayashi, J. Normand, K. Raghavachari, A. Rendell, J. C. Burant, S. S. Iyengar, J. Tomasi, M. Cossi, N. Rega, J. M. Millam, M. Klene, J. E. Knox, J. B. Cross, V. Bakken, C. Adamo, J. Jaramillo, R. Gomperts, R. E. Stratmann, O. Yazyev, A. J. Austin, R. Cammi, C. Pomelli, J. W. Ochterski, R. L. Martin, K. Morokuma, V. G. Zakrzewski, G. A. Voth, P. Salvador, J. J. Dannenberg, S. Dapprich, A. D. Daniels, Ö. Farkas, J. B. Foresman, J. V. Ortiz, J. Cioslowski, and D. J. Fox, *GAUSSIAN 09 (Revision A.02)*, Gaussian, Inc., Wallingford, CT, 2009.
- 54 A. D. Becke, *J. Chem. Phys.*, 1993, **98**, 5648.
- 55 P. J. Stephens, F. J. Devlin, C. F. Chabalowski and C. F. Frisch, *J. Phys. Chem.*, 1994, **98**, 11623–11627.
- 56 W. R. Wadt and P. J. Hay, *J. Chem. Phys.*, 1985, **82**, 284–298.
- 57 P. J. Hay and W. R. Wadt, *J. Chem. Phys.*, 1985, **82**, 270–283.
- 58 P. J. Hay and W. R. Wadt, *J. Chem. Phys.*, 1985, **82**, 299–310.
- 59 A. Schafer, H. Horn and R. Ahlrichs, *J. Chem. Phys.*, 1992, **97**, 2571–2577.
- 60 A. Schafer, C. Huber and R. Ahlrichs, *J. Chem. Phys.*, 1994, **100**, 5829–5835.
- 61 V. Barone, M. Cossi and J. Tomasi, *J. Chem. Phys.*, 1997, **107**, 3210–3221.
- 62 V. Barone, M. Cossi and J. Tomasi, *J. Comput. Chem.*, 1998, **19**, 404–417.
- 63 V. S. Miertus, E. Scrocco and J. Tomasi, *J. Chem. Phys.*, 1981, **55**, 117–129.
- 64 J. Tomadi, B. Mennucci and E. Cancès, *J. Mol. Struct.*, 1999, **464**, 211–226.
- 65 *SAINT, version 4.6A*, Bruker Analytical X-ray System, Madison, WI, 1997–2007.
- 66 *SADABS. Bruker Nonius area detector scaling and absorption correction, V2.10*, Bruker AXS Inc., Madison, WI, 2003.
- 67 *SIR97*: A. Altomare, M. C. Burla, G. Cammelli, M. Cascarano, C. Giacovazzo, A. Guagliardi, A. G. G. Moliterni, G. Polidori and A. Spagna, *J. Appl. Crystallogr.*, 1999, **32**, 115–119; *SIR92*: A. Altomare, G. Cascarano, C. Giacovazzo and A. Guagliardi, *J. Appl. Crystallogr.*, 1993, **26**, 343–350.
- 68 *SHELXTL, Version 5.1*, Bruker AXS Inc., Madison, WI, 1997.
- 69 *TWINABS. Bruker Nonius scaling and absorption for twinned crystals – V2008/2*, Bruker AXS Inc., Madison, WI, 2008.